Catalysis Letters 20 (1993) 169–178



# The role of carbon dioxide in the oxidative dimerization of methane over Li/MgO

Kent Coulter and D. Wayne Goodman [1]

*Department of Chemistry, Texas A&M University, College Station, TX 77843-3255, USA*

Received 17 January 1993; accepted 30 April 1993

$CO_2$ is strongly adsorbed on Li/MgO as a surface carbonate and desorbs concomitantly with Li with an activation energy of desorption of 210 kJ/mol. The $C_2$ product is strongly influenced by the presence of $CO_2$, 0.5 Torr being sufficient to substantially lower the rate of $C_2$ production and to establish an activation energy for reaction of 210 kJ/mol. In the absence of $CO_2$, the activation energy of $C_2$ production falls to 105 kJ/mol.

**Keywords**: Methane coupling; lithium–magnesium oxide; carbon dioxide inhibition

## 1. Introduction

Considerable research on the oxidative dimerization of methane has addressed the fundamental issues related to the reaction mechanism. However, controversy still exists regarding the active sites [1,2], the rate limiting step [3,4], the mechanism for $CO_x$ formation [5,6] and the role of $CO_2$ in altering the reaction mechanism [7,8]. The elucidation of these issues is handicapped by the difficulties and limitations associated with probing this reaction at the required high temperatures (950–1050 K). Further improvements in existing catalysts or the discovery of significantly better catalysts will depend, to a large extent, upon the development of a comprehensive and detailed understanding of the catalytic material and the reaction mechanism.

Detailed kinetic studies have been performed on a few catalysts including Sr/$La_2O_3$ [9] and Li/MgO [10,11] from which generalized rate laws and mechanisms have been fashioned for each of these respective catalysts. A mechanism proposed for the lithium promoted magnesium oxide involves the dissociative chemisorption of oxygen,

$$O_2(g) + 2S + 2e \rightleftharpoons 2O_s^- , \quad (1)$$

[1] To whom correspondence should be addressed.

followed by a rate-limiting step for $CH_4$ activation on active $O^-$ surface sites ($O_s^-$),

$$CH_4(g) + O_s^- \rightarrow CH_3(ads) + O_sH^- . \tag{2}$$

The methyl radicals formed in this step then either couple to form ethane

$$CH_3(ads) \rightarrow CH_3(g) , \tag{3}$$

$$2CH_3(g) \rightarrow C_2H_6 , \tag{4}$$

or oxidize to form CO and $CO_2$,

$$CH_3(ads) \rightarrow CO, CO_2 . \tag{5}$$

From this mechanism a rate law has been proposed for the formation of methyl radicals [9],

$$\frac{d(CH_3\cdot)}{dt} = \frac{k_2 K_1^{1/2}[O_2]^{1/2}[CH_4]}{1 + K_1^{1/2}[O_2]^{1/2}} . \tag{6}$$

This picture is supported by pressure and temperature dependent studies obtained in the 1–100 mTorr (1 Torr = 133.3 kPa) pressure range [11]. In these low pressure experiments an activation energy of 88 kJ/mol was observed, in good agreement with the value of ~ 105 kJ/mol [12] calculated for hydrogen abstraction from methane on either LiO or a $LiO(Mg_4O_5)$ cluster to form $CH_3\cdot$ radicals.

This mechanism proposed by Amorebieta and Colussi fails for higher reaction pressures (760 Torr) and for reactant mixtures that are not fuel rich ($CH_4/O_2 < 10$) [13]. For higher pressures and fuel deficient conditions, the activation energies increase with increasing total pressure and increasing $O_2$ concentrations. For Sr/$La_2O_3$, Feng and Gutman [9] associate this increase in activation energy with an increase in the coverage of surface oxygen. The apparent activation energy observed was proposed to consist of an intrinsic component plus the activation energy for oxygen desorption [9].

Xu et al. [7] attribute the failure of Amorebieta's and Colussi's rate law to poisoning of the oxidative coupling reaction by $CO_2$ [7]. Carbon dioxide has been shown to block adsorption of the reactants thereby lowering the activity and altering the activation energy [8]. The revised rate equation includes $K_{CO_2}[CO_2]$ in the denominator of eq. (6) with the apparent activation energy given as

$$E_a = E_i + \Delta H_{CO_2} , \tag{7}$$

where $E_i$ is the intrinsic activation energy of reaction and $\Delta H_{CO_2}$ is the activation energy for desorption of $CO_2$.

Thin-film Li/MgO catalysts have been shown to be excellent models of the high surface area powders used in the oxidative dimerization reaction [14]. Agreement between the turnover frequencies and activation energies of the thin-film and powder MgO and Li/MgO catalysts indicates that the adsorptive and catalytic

properties of the thin-film models reproduce those of the powders. The utilization of thin-film catalysts allows the use of an array of surface science techniques to investigate these materials. For example, recent studies of the oxidative coupling of methane over thin-film MgO and Li-promoted MgO have provided information about the active sites that could not have been obtained on the bulk catalysts [1]. A correlation between $C_2$ production and the presence of F-type defects (oxygen vacancies containing two electrons) on the Li/MgO thin-film catalyst indicates that the active sites for this reaction are likely F centers in the near-surface region.

In this article, the effects of $CO_2$ partial pressure and reaction temperature for the oxidative coupling of methane on model Li/MgO thin films (10 wt% Li, $\sim$ 20 Å) are reported. The results indicate that the coupling reaction can be carried out in the absence of gas-phase oxygen subsequent to pretreatment of the catalyst in oxygen at 1200 K. Carbon dioxide desorption is shown to be the rate-determining step at high $CO_2$ partial pressures, with the apparent activation energy of reaction markedly decreasing as the partial pressure of $CO_2$ is lowered.

## 2. Experimental

The experiments were carried out on a combined UHV/reactor cell system equipped with Auger electron spectroscopy (AES), temperature programmed desorption (TPD) and dosing capabilities for both gases and metals. The catalyst could be transferred via a double-stage differentially pumped sliding seal from the UHV chamber ($1.0 \times 10^{-10}$ Torr) to a static reactor capable of reaction pressures up to 1000 Torr. All reaction products were analyzed with gas chromatography (GC) utilizing flame ionization detection and a methanizer for $CO_x$ detection. A detailed description of the apparatus can be found elsewhere [15].

The thin-film Li/MgO catalyst was prepared by co-depositing Li and Mg onto a Pt(100) single crystal at room temperature in a background ($5.0 \times 10^{-7}$ Torr) of oxygen. Magnesium deposition was achieved using thermal evaporation from a high purity Mg ribbon wrapped around a tungsten filament. Lithium was deposited onto the surface using a SAES GETTERS source. The dosers were mounted 1.3 cm apart and were 2.5 cm from the sample during dosing. The metal flux was monitored with a mass spectrometer mounted 5 cm from the sources. The evaporation rate of each metal was determined by a combination of TPD and AES measurements; the procedure is described in detail elsewhere [16].

Following preparation and characterization in the UHV chamber, the $\sim$ 20 Å thin-film Li/MgO catalyst was transferred to the reaction cell for activation. The activation process consisted of heating to 1200 K in 1–10 Torr of oxygen for 1–10 min. Subsequently the sample was retracted into the UHV chamber for post-activation analysis using AES.

Catalytic experiments were run in the reactor at temperatures ranging from 950 to 1010 K and total pressures of 1 to 25 Torr. The temperature dependent experi-

ments were typically run at a $CH_4$ : $O_2$ ratio of 10 with a total pressure of 11 Torr. For the $CO_2$ experiments a $CH_4$ : $O_2$ ratio of 10 was used. All reactions were carried out with conversions of less than 1% methane; ethane, CO and $CO_2$ were the major products.

Surface analysis with AES utilized the prominent $Mg^{2+}$ ($L_{23}VV$) transition at 32.0 eV and the $O^{2-}$ (KLL) transition at 505.0 eV. Interference from the $Li^+$ (KLL) transition was taken into account as described by Wu et al. [16]. The TPD studies were carried out with a shielded mass spectrometer to eliminate interference from background desorption processes. Typical heating rates were 5 K/s with a heating range of 300–1300 K.

## 3. Results

Fig. 1 shows the results of a series of reactions with methane (20 Torr) as the only reactant following activation of the Li/MgO catalyst in 1 Torr of $O_2$ at 1200 K. The selectivity of the catalyst as a function of reaction time is displayed. An initial increase in the $C_2$ selectivity was observed during the first few minutes, after which the rate remained essentially constant. A significant shift from $CO_2$ to $C_2$ as the dominate product in the absence of oxygen is apparent; however, it should be noted that the methane conversion in all cases was $<1\%$. The $CO_2$ product concentration, although relatively low, was not zero. AES post-reaction analysis indicated no carbon accumulation on the surface and a small decrease in the oxygen concentration with reaction time. For catalysts with no oxygen pretreatment, no

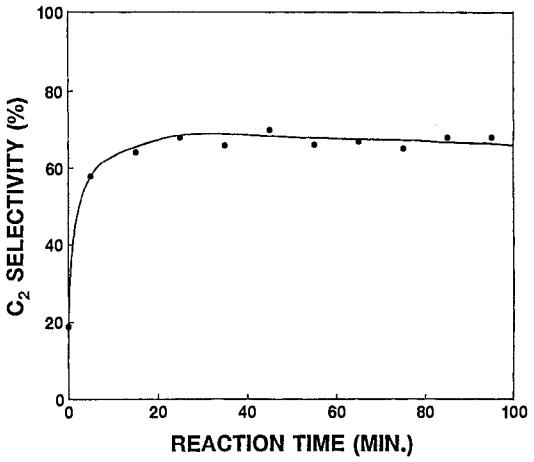


Fig. 1. $C_2$ to $CO_2$ selectivity in the absence of oxygen as a function of reaction time following catalyst activation at 1200 K for 5 min in 2 Torr $O_2$. Reactions were carried out at 990 K in 20 Torr of methane.

$C_2$ products were detected, and no changes were indicated by AES in the catalyst surface with reaction time.

An Arrhenius plot of $C_2$ production at pseudo-steady-state (40–80 min) in the absence of oxygen is shown in fig. 2. The activation energy of fig. 2 corresponds to 140 kJ, considerably lower than the 210 kJ reported for a $CH_4 : O_2$ ratio of 4 at a comparable total pressure over this catalyst [14]. At 990 K in an oxygen-free environment, the $C_2$ turnover frequency (TOF) is $1.4 \times 10^{-2}$ molecules/site s (site $\approx 10^{17}/cm^2$). The TOF recorded in the absence of oxygen is somewhat higher than the value ($9.0 \times 10^{-3}$ molecules/site s) observed for a $CH_4/O_2$ ratio of 4 [14].

As discussed above, the partial pressure of $CO_2$ plays a key role in altering the catalyst and the reaction mechanism. One of the effects of carbon dioxide is to stabilize the lithium on the MgO surface as shown in fig. 3. The TPD spectrum for lithium deposited in a $CO_2$-free environment (fig. 3a) has a desorption maximum at 700 K whereas the desorption spectrum obtained following lithium deposition in a $CO_2$ background (fig. 3b) exhibits a maximum at 1050 K with a shoulder at 875 K. Xu et al. [7] have identified this stable form of Li as a $Li_2CO_3$ phase that is modified by MgO.

$CO_2$ desorption from Li/MgO following a saturation exposure of $CO_2$ is shown in fig. 4. The desorbing $CO_2$ (mass 44) follows in concert the Li desorption observed in fig. 3b. A kinetic analysis of the TPD profile suggests an activation energy of 240 kJ for $CO_2$ desorption from the 875 K feature. The similarities in the activation energies for the desorption of $CO_2$ from this 875 K feature and the oxidative coupling reaction with significant $CO_2$ pressure ($\sim$ 210 kJ) strongly suggest that desorption of $CO_2$ from this particular adsorbed species is the rate-limiting step under these reaction conditions.

To directly address the role of $CO_2$ in altering the available reactive sites at the

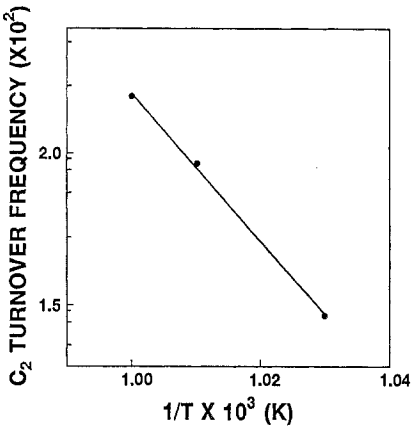


Fig. 2. A plot of the turnover frequency versus inverse reaction temperature for methane coupling (20 Torr methane) in the absence of gas-phase oxygen following pretreatment of the catalyst in 2.0 Torr $O_2$ at 1200 K. The apparent activation energy is 140 kJ/mol.

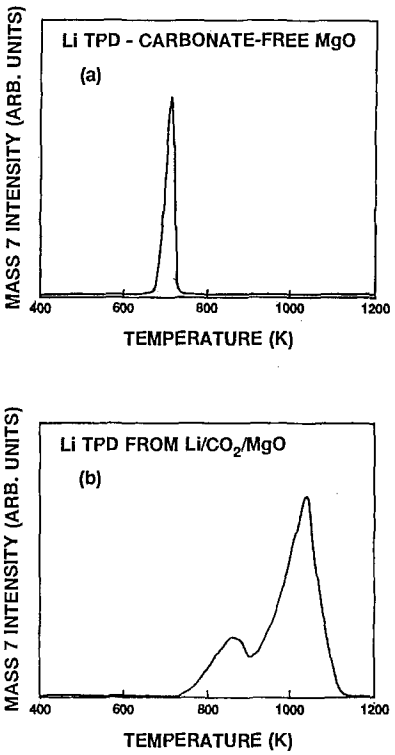


Fig. 3. (a)Temperature programmed desorption spectrum of lithium (mass 7) on MgO. (b) Temperature programmed desorption spectrum of lithium (mass 7) from MgO subsequent to deposition in a background of carbon dioxide.

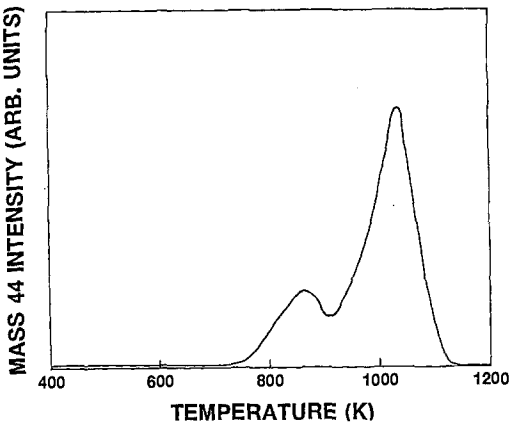


Fig. 4. Temperature programmed desorption spectrum of $CO_2$ (mass 44) from Li/MgO.

Li/MgO surface, the reaction was carried out in a $CO_2$-free environment. This was made possible by immersing the reactor cell in a liquid $N_2$ bath. At 77 K, the $C_2$ and $CO_2$ products were immediately adsorbed onto the walls of the reactor, thus maintaining their partial pressures in the reaction mixture essentially at zero. An Arrhenius plot of the $C_2$ production in the cold wall reactor, displayed in fig. 5, yields an apparent activation energy of 105 kJ. This value likely corresponds to the intrinsic activation energy of the hydrogen abstraction step *plus* the activation energy for the active site formation. The active site as discussed in ref. [1], is believed to be an F-type defect center.

The effect of $CO_2$ partial pressure on the $C_2$ production is shown in fig. 6. The $C_2$ formation rate falls rapidly with an increase in the partial pressure of $CO_2$ as low as 0.5 Torr. These results are in agreement with the earlier results of Korf et al. [8], and the more recent results of Xu et al. [7], where $CO_2$ was found to inhibit the production of $C_2$ as well as methyl radical formation. For all concentrations of $CO_2$ the apparent activation energy for reaction was 200–225 kJ/mol.

## 4. Discussion

Carbon dioxide effects on the Li/MgO catalyst appear to be twofold. First, it stabilizes the lithium promoter as shown in fig. 3. Secondly, however, $CO_2$ in the form of a carbonate or carbonate-like species inhibits the reaction as seen in fig. 6. The similarities between the activation energy of desorption of the 875 K species of fig. 4 and the activation energy of the dimerization reaction with high concentrations of $CO_2$ suggest a dominant inhibiting effect. These results are consistent with the rate-limiting step for the coupling reaction in the presence of high concentrations of $CO_2$ being the desorption of $CO_2$. $CO_2$ desorption, in turn, frees an active site for the dissociative adsorption of methane.

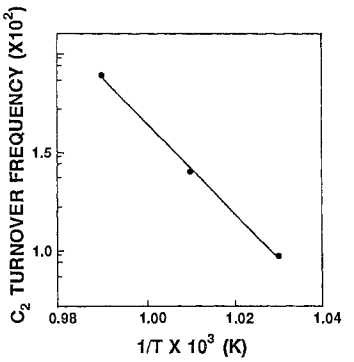


Fig. 5. An Arrhenius plot of $C_2$ production in a cold (77 K) wall reactor with $P_{CH_4} = 20$ Torr and $P_{O_2} = 1$ Torr. The apparent activation is 105 kJ/mol.

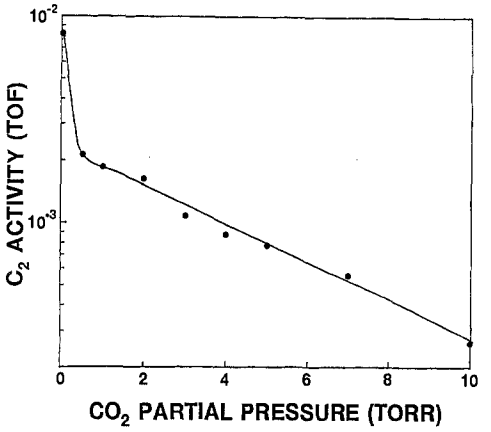


Fig. 6. $C_2$ production as a function of $CO_2$ partial pressure in the initial reactant mixture. $P_{CH_4}$ = 10 Torr, $P_{O_2}$ = 1 Torr and $T$ = 990 K.

If $CO_2$ desorption under these conditions is the rate-limiting step, then the reduction in the activation energy observed for the cold wall reaction of fig. 5 can be explained by a significant shift in the $CO_2$ adsorption/desorption equilibrium. This shift yields a surface that is essentially free of adsorbed $CO_2$. Accordingly, the apparent activation energy under these conditions of 105 kJ is consistent with the rate-determining step having changed to the hydrogen abstraction step. This step has been shown to have an activation energy of ~ 90 kJ/mol on Li/MgO [11] and on $Sr/La_2O_3$ [9]. The cold wall reaction in this study can be compared to previous studies [17] at low pressure since in both cases the concentration of $CO_2$ is sufficiently low such that the surface coverage of $CO_2$ is negligible.

Reactions carried out with $CO_2$ in the reactant mixture clearly show that $CO_2$ adsorption must be incorporated into the reaction rate law. With increasing partial pressures of $CO_2$, the $C_2$ production falls, consistent with an increase in the surface $CO_2$ coverage. The activation energy is invariant at approximately 210 kJ/mol, independent of the $CO_2$ partial pressure, as long as this pressure is >0.5 Torr.

From the present results, it is evident that a realistic rate law of methane activation must incorporate competitive adsorption of $CH_4$ and $CO_2$. The rate law proposed by Xu et al. [7], accounts for the pressure dependence in $CO_2$ by adding the adsorption equilibrium for $CO_2$ to the rate law (6) denominator

$$\frac{d[CH_3]}{dt} = \frac{k_2[CH_4]K_1^{1/2}[O]_2^{1/2}}{1 + K_1^{1/2}[O_2]^{1/2} + K_{CO_2}[CO_2]}. \tag{8}$$

This rate law with respect to $CO_2$ is consistent with the results found in this study.

Analysis of the rate law (8) with the inclusion of the $CO_2$ term is informative. For the reaction with oxygen, the concentration of $CO_2$ increases with an increase

in the methane conversion, thus shifting the rate limiting step from C–H bond cleavage to $CO_2$ desorption. Removal of gas-phase oxygen clearly improves the $C_2$ yield of the oxidative dimerization reaction, suggesting that cycling the catalyst in oxygen at high temperatures to generate active sites followed by a second step in which the pretreated catalyst is reacted with methane, could maximize the $C_2$ selectivity. Work is currently in progress to explore this reaction sequence.

## 5. Conclusions

The dependence of the oxidative coupling reaction on the partial pressures of carbon dioxide has shown that the rate-limiting step is dependent on the $CO_2$ coverages on the catalyst. At low $CO_2$ partial pressures the activation energy for the dimerization reaction indicates that the rate-limiting step is C–H bond cleavage. Under conditions of relatively high $CO_2$ partial pressures the rate-determining step is $CO_2$ desorption based upon the similarities between the desorption activation energy of $CO_2$ and the activation energy for $C_2$ formation.

## Acknowledgement

We acknowledge with pleasure the support of this work by the Gas Research Institute.

## References

[1] M.C. Wu, C.M. Truong, K. Coulter and D.W. Goodman, J. Catal., in press.
[2] D.J. Driscoll, W. Martir, J.X. Wang and J.H. Lunsford, J. Am. Chem. Soc. 107 (1985) 58.
[3] N.W. Cant, C.A. Lukey, P.F. Nelson and R.J. Tyler, J. Chem. Soc. Chem. Commun. (1988) 766.
[4] A. Ekstrom and J.A. Lapszewicz, J. Phys. Chem. 93 (1989) 5230.
[5] J.A. Roos, S.J. Korf, R.H.J. Veehof, J.G. Van Ommen and J.R.H. Ross, Appl. Catal. 52 (1989) 131.
[6] A. Ekstrom and J.A. Lapszewiecz, J. Am. Chem. Soc. 111 (1989) 8515.
[7] M. Xu, C. Shi, X. Yang, M.P. Rosynek and J.H. Lunsford, J. Catal., submitted.
[8] S.J. Korf, J.A. Roos, N.A. deBruijn, J.G. Van Ommen and J.R.H. Ross, J. Chem. Soc. Chem. Commun. (1987) 1433.
[9] Y. Feng, J. Niiranen and D.J. Gutman, J. Phys. Chem. 95 (1991) 6558;J. Phys. Chem. 95 (1991) 6564.
[10] J.B. Kimble and J.H. Kolts, Energy Progress 6 (1986) 226.
[11] V.T. Amorebieta and A.J. Colussi, J. Phys. Chem 92 (1988) 4576.
[12] K.J. Børve and L.G.M. Petterson, J. Phys. Chem. 95 (1991) 7401.
[13] T. Ito, J.X. Wang, C.-H. Lin and J.H. Lunsford, J. Am. Chem. Soc. 107 (1985) 5062.

[14] K. Coulter and D.W. Goodman, Catal. Lett. 16 (1992) 191.
[15] J. Szanyi and D.W. Goodman, in preparation.
[16] M.C. Wu, J.S. Corneille, C.A. Estrada, J.W. He and D.W. Goodman, Chem. Phys. Lett. 182 (1991) 472.
[17] C. Mirodatos and G.A. Martin, *Proc. 9th Int. Congr. on Catalysis*, Vol. 2, Calgary 1988, eds. M.J. Phillips and M. Ternan (Chem. Inst. of Canada, Ottawa, 1988) p. 899.
[18] C.-H. Lin, T. Ito, J.-X. Wang and J.H. Lunsford, J. Catal. 111 (1988) 302.